frontiers | Frontiers in Environmental Science

ORIGINAL RESEARCH
published: 11 May 2022
doi: 10.3389/fenvs.2022.894240

Efficiency of Carbon-Based Electrodes on a Microbial Electrolysis System for the Treatment of Bilge Water

Georgia Gatidou[1]*, *Marios Constantinou*[2], *Loukas Koutsokeras*[2], *Ioannis Vyrides*[1]* and *Georgios Constantinides*[2]

[1]Laboratory of Environmental Engineering, Department of Chemical Engineering, Cyprus University of Technology, Lemesos, Cyprus, [2]Nano/Micro Mechanics of Materials Laboratory and Research Unit for Nanostructured Materials Systems, Department of Mechanical Engineering and Materials Science and Engineering, Cyprus University of Technology, Limassol, Cyprus

A coupled Microbial Electrolysis Cell (MEC) – Anaerobic Granular Sludge (AGS) system was settled to investigate for the first time the ability of various carbon-based electrodes to enhance biodegradation of real bilge water (BW) and increase methane generation as an emerging technology for converting organic matter into value-added products. Results revealed that the performance of the three types of electrodes named carbon foam (CF), carbon cloth (CC) and three-dimensional graphene foam (3DG), was both time and organic load content dependent during the experimental cycles. Cumulative CH_4 generation reached 235 mL in just 13 days after feeding the AGS with 50% of BW and application of 1.0 V at 3DG electrodes, followed by CC electrodes (148.3 mL). CF proved to be more resistant in higher BW concentration showing a sufficient performance of 1 month. However, in the third cycle, the performances of MECs containing 3DG and CC were higher compared to the CF and the control. Over the first cycle, the soluble Chemical Oxygen Demand (sCOD) removal was found to be around 70% to all MECs, and this value was around 10% higher than the control. Among the different Volatile Fatty Acids (VFAs), acetic acid was identified in the highest concentration in the first cycle, whereas propionic acid was detected in the second and third cycles. Microbial profile analysis showed that *Methanobacterium* and *Desulfovibrio* had substantially higher abundances in the cathodes than in the suspended anaerobic sludge. An X-ray diffraction (XRD) investigation of the used electrodes pointed out the formation of various crystalline compounds on their surface, which were different for the anode and cathode.

Keywords: bilge water, carbon foam, carbon cloth, 3D graphene foam, microbial electrolysis cell, anaerobic treatment

OPEN ACCESS

Edited by:
Narcis Pous,
University of Girona, Spain

Reviewed by:
Marco Zeppilli,
Sapienza University of Rome, Italy
Zhao Yuxiao,
Shandong Academy of Sciences, China

***Correspondence:**
Georgia Gatidou
ggatid@env.aegean.gr
Ioannis Vyrides
ioannis.vyrides@cut.ac.cy

Specialty section:
This article was submitted to Water and Wastewater Management, a section of the journal Frontiers in Environmental Science

Received: *11 March 2022*
Accepted: *20 April 2022*
Published: *11 May 2022*

Citation:
Gatidou G, Constantinou M, Koutsokeras L, Vyrides I and Constantinides G (2022) Efficiency of Carbon-Based Electrodes on a Microbial Electrolysis System for the Treatment of Bilge Water. Front. Environ. Sci. 10:894240. doi: 10.3389/fenvs.2022.894240

INTRODUCTION

Bilge water is the wastewater accumulated in a ship's bilge. It consists of seawater and several types of wastes such as cleaning solvents, detergents, grease, oil additives, heavy metals, hydrocarbons, *etc.* (Vyrides et al., 2018) and is considered a recalcitrant wastewater (Mazioti A. A. et al., 2021). Its chemical composition differs from ship to ship and among days within the same ship (Tiselius and Magnusson, 2017). The characteristics of BW are also affected by ship's operations, equipment

performance and repairs (McLaughlin et al., 2014). Among other things, high values of COD (up to 15 g L^{-1}), salinity (up to 35 g L^{-1}) or oil content (up 2953 mg L^{-1}) have been reported in the literature (Vyrides et al., 2018). These properties make BW treatment very difficult or unsatisfactory to meet international regulations regarding BW discharges by applying conventional treatment methods. Therefore, finding alternative economic and environment-friendly methods to enhance treatment effectiveness is needed.

So far, an alternative method for bilge water treatment against physicochemical and biological processes is the bioelectrochemical process. Hwang et al. (2019) used single chamber microbial fuel cells (MFCs) with *Pseudomonas putida* ATCC 49128 for synthetic bilge water biodegradation with simultaneous electricity generation. The COD removal was 71% in 20 days. Moreover, they investigated the effect of surfactant addition on the biodegradation of bilge water using an MFC. Their results showed that the addition of surfactant substantially improved the biodegradation of bilge water. Similarly, in another study, Hwang et al. (2021) used single and double-chamber microalgal fuel cells (SMAFC and DMAFC) capable of generating energy with a novel microalgal strain (*Chlorella sorokiniana*) that was isolated from oily wastewater to treat synthetic bilge water. Both SMAFC and DMAFC removed 67.2–77.4% of soluble COD from an initial 5576.5 ± 166.5 mg COD. Mei et al. (2019) assessed an integrated MFC with an electrocoagulation process to treat synthetic bilge water (2029 ± 61 mg L^{-1}). In that study, three MFCs were connected in series using as a power source an electrocoagulation cell (ECC) for an onboard system for bilge water treatment. The results showed that acetate-fed or municipal waste MFC stacks can effectively provide enough energy to power ECC operation for bilge water treatment. The MFCs-ECC system removed successfully 93% of oil content; during a 4-h treatment, the COD of bilge was reduced to 347 ± 15 mg L^{-1} (83% removal) when powered by MFC series stack. Recently, Gatidou et al. (2022) examined real bilge water treatment using a microbial electrolysis cell (MEC) containing iron rod electrodes. After gradual biomass acclimatization, sCOD removal up to 70% was identified in this study. Furthermore, MEC operation at 1V resulted in better performance than the control or the operation at 2 V (Gatidou et al., 2022).

In MECs, electroactive microorganisms using an electrode surface as an external electron acceptor oxidize organic compounds producing protons, CO_2 and electrons. Electrons generated by this electrogenic biofilm are transferred *via* extracellular electron transport (EET) to the anode and subsequently to the cathode through an externally applied electrical circuit (Zeng et al., 2016). The conversion of CO_2 to CH_4 in the cathode is achieved through direct or indirect (H_2 mediator) pathways (Choi and Sang, 2016).

One of the key parameters of a MEC system is the selection of the electrode material because it determines the electrons transfer between exoelectrogens and electrodes which will take place (Mier et al., 2021). High conductivity, specific surface area and biocompatibility are considered core characteristics for achieving high rates of methanogenesis and organic load removal (Mier et al., 2021). Up to now, to the best of our knowledge, there is only one study regarding the application of the MEC-AD process for the treatment of real BW using commercial iron electrodes (Gatidou et al., 2022). However, colonization of metal surfaces such as iron by microbes may speed metallic corrosion in an aqueous environment (Krishnamurthy et al., 2013), leading to reduced performance of the MEC system. Thus, carbon-based materials like carbon cloth, carbon felt, graphite particles and others are often used instead due to their satisfactory stability in the microbial inoculum, great electrical conductivity and low toxicity (Mier et al., 2021). Unfortunately, simple carbon materials present poor biocompatibility and poor electrocatalytic activity and, for this reason often are modified to improve their performance (Mansoorian et al., 2020). Up to now, there are no data available regarding the application of carbon-based electrodes same or similar to those used in the study on the treatment of real BW by MEC coupled with AGS. Therefore, the current work, aimed to examine the efficiency of these types of electrodes on the biodegradation of real bilge water during batch experiments and using anaerobic granular sludge as an inoculum. More precisely electrodes of carbon foam (CF), carbon cloth (CC) and three-dimensional graphene foam (3DG) were produced and examined. The application of 1.0 V of external potential was investigated in order to enhance CH_4 production and dCOD elimination for three consecutive batch cycles having total duration of almost 2 months (52d).

MATERIALS AND METHODS

Semi-Batch Experiment

Anaerobic granular sludge used as inoculum, was provided from a full-scale upflow anaerobic sludge blanket (UASB) treating dairy wastewater (Charalambides Christis Ltd., Cyprus). Before its use, the sludge was sieved (1 mm), washed with distilled water and transferred into a duran glass bottle (1 L). Then, it was flushed with CO_2 (99.99%) for 5 min to achieve anaerobic conditions and placed in a shaking incubator for a week at 34°C in order to activate the biomass. Real BW was collected from Ecofuel Ltd. Company (Zygi, Cyprus). The characteristics of pre-settled BW were as follows: pH: 7.5, COD: 2.9 g COD L^{-1}, total Solids (TS): 9557 mg L^{-1}, volatile solids (VS): 3053 mg L^{-1}, conductivity: 16.3 $mScm^{-1}$, salinity as g L^{-1} NaCl: 9.9 g L^{-1}.

Batch lab-scale experiments were performed using four 1 L glass reactors as single chamber MEC (working volume of 0.7 L). The four reactors were set up and operated simultaneously as follows: R0 without electrodes inside which served as the control (R0-C), R1 containing carbon foam CF electrodes (R1-CF), R_2 containing carbon cloth CC electrodes (R2-CC) and R3 containing 3DG graphene foam electrodes (R3-3DG). Anode and cathode in the different MECs constituted by the same material. The performance of the MECs was studied by applying a constant potential of 1.0 V using a DC power supply (GW-Instek, Taiwan). Each reactor was fed with 50 g of AGS and BW at different concentrations; cycle A: 50%, cycle B: 75% and cycle C: 75% BW. The remaining volume was filled with anaerobic medium (Angelidaki et al., 2009) and the pH was

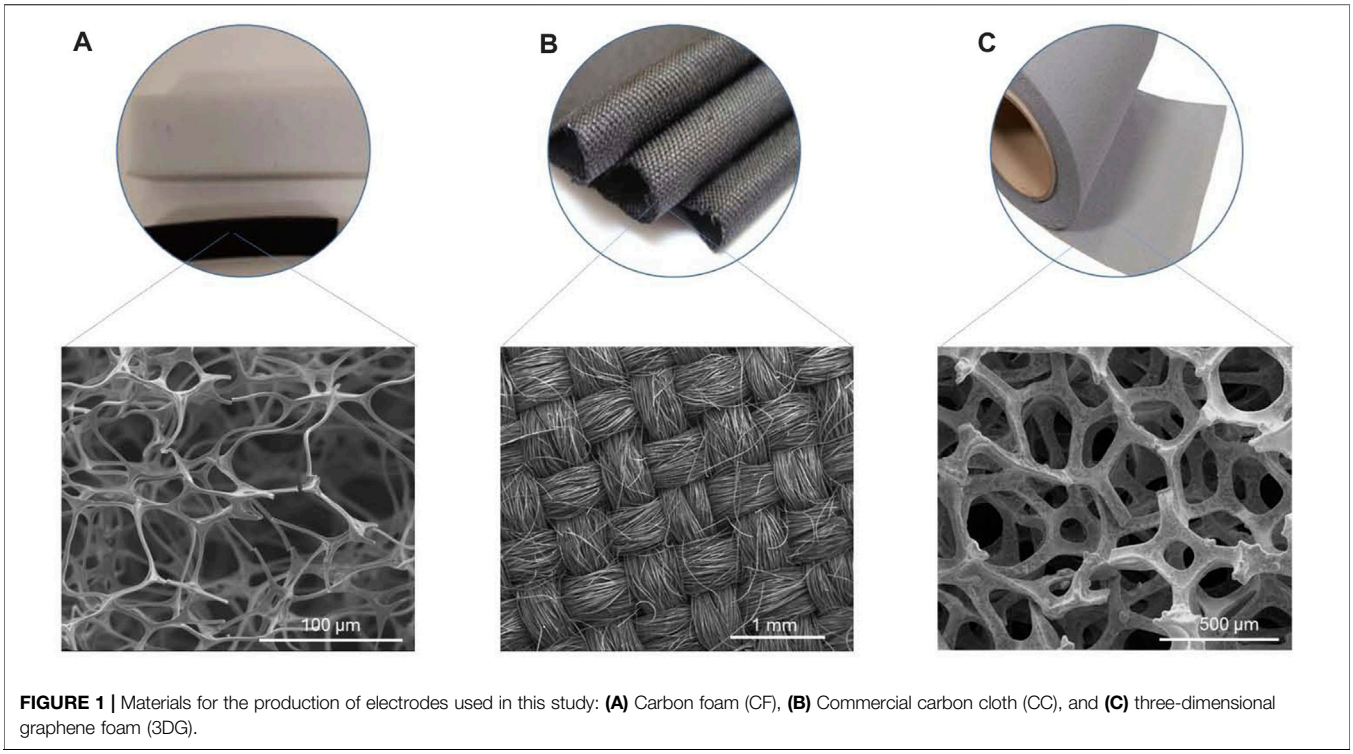

FIGURE 1 | Materials for the production of electrodes used in this study: **(A)** Carbon foam (CF), **(B)** Commercial carbon cloth (CC), and **(C)** three-dimensional graphene foam (3DG).

adjusted to 7.5. Finally, CO_2 was flushed inside (5 min) the bioreactors only at the beginning of each cycle, for achieving anaerobic conditions and the reactors were placed at 34 °C. In total, three consecutive batch cycles were run for almost 2 months (52d) (cycle A: 13d, cycle B: 19d and cycle C: 21d). Throughout the experiments the output voltage in MEC-AD was recorded every 5 min by a data acquisition system (Keithley 2700) connected to a computer.

Carbon-Based Electrodes

Carbon based electrodes used in this study were produced with commercially available materials that were used as received (CC) or after processing/modification (CF and 3DG). Carbon foam CF electrodes (CF) were produced through a pyrolysis process of a commercially available melamine-based foam (Basotect G^+) using a thermal deposition system activated chemical vapor deposition (TCVD) reactor. Small pieces of the melamine-based foam were heated in a quartz tube with a rate of 5°C min^{-1} to 900 °C, kept at that temperature for 6 h and subsequently cooled to room temperature. The whole pyrolysis process was performed under nitrogen flow of 50 sccm in reduced pressure, achieved by a dry scroll pump. Commercial carbon cloth (CC) was purchased from Zoltek Corporation (United States) having characteristics of plain weave PWO3 and a square shape 400 x 400 mm^2. For the current experiments pieces of 20 × 60 mm^2 were cut and converted into electrodes with no additional material processing.

The synthesis of three-dimensional graphene foam (3DG) was performed using a commercial nickel foam (MTI Corporation, USA) as template material for catalytic growth of graphene. The template nickel foam material had a purity of about 99.9% and the number of pores per inch (PPI) were about 80 – 110 with an average pore diameter of approximately 250 μm. Each electrode of nickel foam was prepared in the form of a roll with a plane surface area of 20 × 60 mm^2 and a thickness of 1.6 mm, and its weight was approximately 545 mg. Prior to the graphene formation process, the nickel foam samples were degreased ultrasonically in ethanol and dried at room temperature before placed into the TCVD reactor. After inserting the nickel sample into the TCVD reactor, immediately the system was evacuated for 20 min to reach a pressure of 0.004 Torr. After the 20 min period the reactor was purged with 25% hydrogen (H_2) in argon gas flow (a total mixture flow of) 265 sccm for additional 20 min. The system was then heated to 1000 °C with a ramping rate of 40°C min^{-1}. When the temperature of 1000 °C was reached an additional 20 min waiting at that temperature was carried out for temperature stabilization. Graphene synthesis then followed by introducing CH_4 molecules into the system with a rate of 50 sccm for 30 min, while the initial 25 % H_2 in argon gas mixture was still flowing into the system. The completion of synthesis allowed to cool down the chamber to room temperature only with argon flow of 265 sccm. All three materials used in electrodes production in this study together with Scanning Electron Microscopy (SEM) images of their respective microstructures are presented in **Figure 1**.

Analysis of Electrodes

At the end of cycle C used electrodes were dried and prepared for characterization d. Used cathodes and anodes were studied by XRD measurements in a Rigaku Ultima IV diffractometer equipped with a copper tube and operated at 40 kV and 40 mA. The system was configured in parallel beam mode by

a multilayer mirror and patterns were recorded in θ–2θ (Bragg-Brentano) scans using Cu Kα radiation (λ = 0.15419 nm). A fixed graphite monochromator was also used at receiving optics to suppress fluorescence.

Due to the nature (size and shape) of the used electrodes, it was very difficult to achieve proper forms for the XRD scans, which resulted in low signal to noise ratio. Furthermore, the unknown composition of the bilge water made the peak identification a rather challenging process. Thus, the XRD patterns are considered in a qualitative manner and treated as indications for the involved processes between the electrodes and the bilge water.

Microbial Profile Analysis

AGS samples (~250 mg) were collected from bioreactors and electrodes similarly to Gatidou et al. (2022) at the end of cycle C. DNeasy PowerSoil Pro kit (Quiagen, Germany) was used for the total genomic DNA extraction following manufacturers' instructions and the final extracts were analyzed by DNASense Apps Company (Denmark). Analytical description of the used protocol is given in the **Supplementary Material** (Section A. Analytical Methods).

Analytical Methods

Total solids (TS), volatile solids (VS) and sCOD were performed based on Standard Methods (APHA 2005). Composition of produced biogas analysis was achieved by an Agilent Technologies Gas Chromatographer 7820A connected to a Thermal Conductivity Detector (Wilmington, DE, United States) according to Vyrides et al. (2018). Separation of the several gases (H_2, O_2, N_2, CH_4, and CO_2) was performed with a ShinCarbon ST packed column (Restek Corporation, Bellefonte, PA, United States) using argon (1 mL min^{-1}) as a carrier gas and the following column temperature program: 2 min at 60°C, then increase to 160°C with a rate of 20°C min^{-1} and hold for 1 min. The injector and detector were maintained at 125 and 250°C, respectively. The produced volumes of biogas were measured using a 50 mL glass syringe and reported at atmospheric pressure.

Concentrations of VFAs (acetic, propionic, iso-butyric, butyric and valeric acid) were determined by injecting 1 μl of the sample to High-Performance Liquid Chromatographer- UV detector (LC-20AD, Shimadzu, Japan) according to Vyrides and Stuckey (2009). Elution of the compounds was performed isocratically with a flow rate 0.7 mL min^{-1} on a Rezex™ ROA-Organic Acid H+ (8%) (150 × 7.8 mm, Phenomenex) with 5 mM H_2SO_4 at 50°C. The UV detector was set at 210 nm during the analysis.

Calculations

The cumulative methane yield was calculated according to (Charalambous and Vyrides, 2021). The removal efficiency of sCOD was calculated according to **Eq. 1**:

$$\%Removal_{sCOD} = \left(\frac{sCOD_o - sCOD_t}{sCOD_o}\right)x100 \quad (1)$$

Where, COD_0 and COD_t are the major pollutants' concentrations at the start and at the end of the experiment.

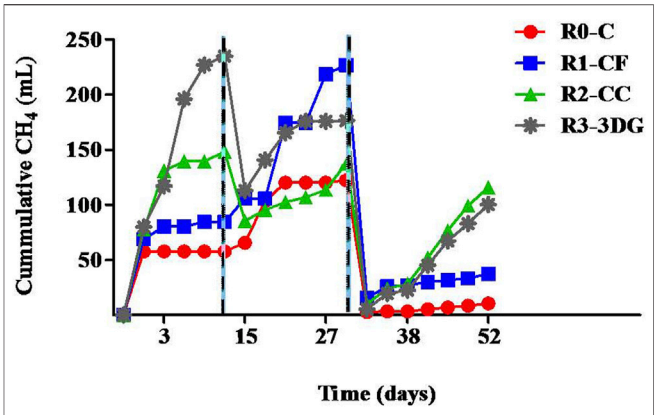

FIGURE 2 | Cumulative methane (mL) produced over time in control (R0-C) and in MECs containing carbon foam (R1-CF), carbon cloth (R2-CC) and 3-dimensional graphene (R3-3DG). Dot lines represent the beginning of the next experimental cycle.

First order kinetic equation was fitted to COD concentration profiles for each reactor and the removal rate constants (k), the half-life values ($t_{1/2}$) and the correlation coefficients (R^2) were calculated as follows (**Eq. 2**):

$$C_t = C_O e^{-kt} \quad (2)$$

Where C_t and C_0 are the COD concentration at time t and t = 0, respectively, (mg L^{-1}), k is the removal coefficient (d^{-1}) and t is the time at the end of each experimental cycle.

GraphPad Prism 5 for Windows software was used for data evaluation.

Current (I) was calculated using the Ohm's law (**Eq. 3**):

$$I = V/R \quad (3)$$

Where V is the applied voltage (V) and R is the resistor connected in the MECs (10 Ω).

The energy efficiency of microbial electrolysis cell was calculated according to Xing et al. (2021) following the **Eq. 4**:

$$\mu E = \frac{(V - V_C) \times \Delta H}{Vm \times \sum_{i=1}^{n} I_i E \Delta_t} \quad (4)$$

Where μE is the energy efficiency of microbial electrolysis cell, Ii is the current (A) of external circuit for microbial electrolysis cell, E is the voltage (V) of MEC, Δt is the digestion time in each cycle (s), V is the methane volume (L) of microbial electrolysis cell, Vc is the methane volume (L) of bioreactor without extranet voltage, ΔH is the upper heating value of methane (890.31 × 10^3 J mol^{-1}), Vm is molar volume of gas at ambient temperature and pressure (22.4 L mol^{-1}).

RESULTS AND DISCUSSION

Methane Production

Cumulative methane production during each running cycle for all reactors is presented in **Figure 2**. According to the results

throughout the experiments, higher methane generation was always detected in MECs than in the control anaerobic bioreactor. After the first operation cycle with diluted 50% real bilge water (cycle A), the cumulative methane was found to be 1.5, 2.6, and 4.1 times higher than the control for R1-CF, R2-CC and R3-3DG, respectively confirming the advantage of using MEC systems for the treatment of recalcitrant wastewater. The 3DG electrodes had the highest performance among the three different electrodes. At the end of cycle A, a total of 235.3 mL methane was produced in the R3-3DG reactor. This volume was about 58 and 179% higher than the measured gas in R2-CC and R1-CF, respectively. Higher methane production in R3-3DG reaction was probably connected with its preeminent properties like high electrical conductivity and/or large accessible surface (Mao et al., 2015) that favor the colonization of this material by microorganisms (Yu et al., 2016). This is also in line with the higher energy efficiency found in R3-3DG compared to other reactors (please *see* section regarding **energy efficiency**) Furthermore, the possible release of nickel ions from the electrode into the liquid phase could also be a possible reason for the higher methane content in the R3-3DG reactor. Nickel (the base of 3DG electrodes) is an essential trace element next to others and plays a critical role in methanogenesis. It is involved in the function of enzymes such as NiFe hydrogenases, carbon monoxide dehydrogenase/acetyl-CoA synthase, hydrogenases, and F420-reducing hydrogenases (Khan et al., 2021). Additionally, the nickel template may be also oxidized, contributing to hydrogen production and, therefore, enhanced hydrogenotrophic methanogenesis.

Estimating the cycle, A, a new feeding was performed on day 13, applying higher organic load content in the reactors. The results indicated that when the concentration of bilge water was increased to 75% (cycle B), methane generation was enhanced in R1-CF reactor and reached 226.7 mL (**Figure 2**) at day 31 (end of cycle B). On the contrary, in R2-CC methane production, although presented an increase, at the end of cycle B, its value fluctuated at the same levels as cycle A. Regarding the R3-3DG reactor, feeding with a higher organic load resulted in about 33% less gas production (176.3 mL) on 31d than cycle A, indicating that this material loses its effectiveness soon enough, probably due to the oxidation of nickel. Nevertheless, the overall methane generation in MECs was still higher than in control. Specifically, it was found to be 12.3, 44.2, and 85.3% increased for R2-CC, R3-3DG and R1-CF, respectively.

Replacement of liquor on day 31 with fresh BW (start of cycle C) resulted in even lower methane generation in all MEC reactors than in previous cycles (**Figure 2**), while in the control bioreactor, the production was negligible. At the end of the experiment (52d), the cumulative methane was 37.5, 115.8 and 100.3 mL for R1-CF, R2-CC and R3-3DG, respectively. Nevertheless, methane production increased R2-CC and R3-3DG, whereas R1-CF reached a steady-state 3 days after the feeding, similar to cycle A. This lower methane production during the last cycle could be due to the biomass's possible weakening and inability to cope with the toxic and high salinity environment for a long time, given that no previous adaptation in saline conditions took place before the beginning of the experiment. As reported in the literature, the existence of high osmotic pressure for an extended period (use of 75% BW from day 13 until 52) may force biomass to consume the organic load for their survival instead of methanogenesis (Vyrides and Stuckey, 2009). Furthermore, the presence of specific pollutants like organic solvents or hydrocarbons often detected in BW may also contribute to reduced methane generation. According to the literature, several authors have reported the existence of different compounds. For instance Vyrides et al. (2018) identified methyl isobutyl ketone and heptane in untreated BW. Similarly, McLaughlin et al. (2014) detected methyl ethyl ketone, while Cazoir et al. (2012).

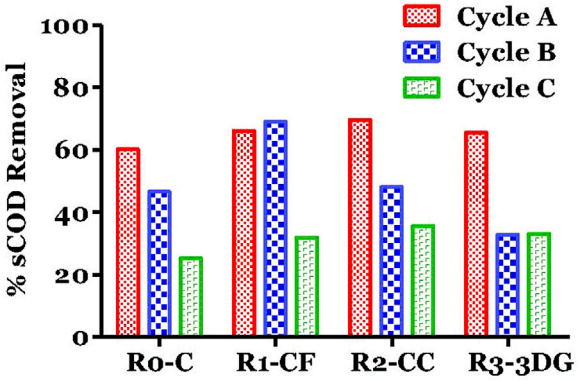

FIGURE 3 | Removal of soluble COD (%) at the end of each experimental cycle A, B and C.

In a recent study, Gatidou et al. (2022) evaluated the performance of commercial iron electrodes in MEC reactors for the treatment of real BW. According to their results, during the first 15 days of the experiment, the cumulative methane in the MEC reactor working at 1 V was negligible although only 25% of BW was used. On the contrary, the results of the current study show that carbon-based electrodes are more effective for the start-up of a MEC system than the commercial iron electrodes.

COD Removal Efficiency

The sCOD removals at the end of each cycle are shown in **Figure 3**. At the end of cycle A the sCOD removal in all MECs found to be similar to all reactors and up to 69.6%. This value was higher than Gatidou et al. (2022) during their cycle A of experiment, considering the double content of BW that was used in the present study (50%). However, the measured values were only about 5–10% higher than the control, indicating a slight improvement in organic load removal due to MEC application. Moreover, the CH_4, as was shown in **Figure 2**, was higher for MEC systems than the control, and this is not in line with the COD results (**Figure 3**). At the end of cycle A, the produced gas corresponded to 26.7, 46,4 and 77.1% of the initial COD for R1-CF, R2-CC and R3-3DG, respectively. This could be due to hydrogen production from water electrolysis and the subsequent utilization by hydrogenotrophic methanogens.

TABLE 1 | First order kinetics (k), half-life ($t_{1/2}$) and correlation coefficients (R^2) values calculated for sCOD concentrations in batch experiments during different feeding cycles.

		Cycle A	
	R1-CF	R2-CC	R3-3DG
k (d^{-1})	−0.087	−0.111	−0.089
$T_{1/2}$ (days)	8.0	6.2	7.8
R^2	0.8654	0.809	0.9099
		Cycle B	
	R1-CF	R2-CC	R3-3DG
k (d^{-1})	−0.078	−0.042	−0.024
$T_{1/2}$ (days)	8.9	16.6	28.8
R^2	0.7027	0.772	0.8418
		Cycle C	
	R1-CF	R2-CF	R3-3DG
k (d^{-1})	−0.023	−0.024	−0.026
$T_{1/2}$ (days)	29.8	29.2	26.2
R^2	0.8346	0.9849	0.8381

During the next cycle, the increase of BW content (75%) seemed to affect the performance of some reactors. According to the results, the sCOD removal was significantly lower in R3-3DG and R2-CC than cycle A, with values as high as 32.9 and 48%, respectively on day 32 (end of cycle B), revealing a possible shock of microorganisms due to the higher salinity of the new feeding. As reported in the literature (Ma et al., 2020; Ahmadi et al., 2017), the lack of acclimation of non-halophilic biomass to high saline environments can result in gradual cell dehydration and enzyme deactivation to the osmotic difference, which can even lead to lower removal of organic loads. On the contrary, the COD removal in R1-CF remained high (69%), possibly due to higher porosity of carbon foam material (100 pores cm^{-1}) compared to carbon cloth and 3D-graphene (39 porescm^{-1}), which led to more significant adsorption of the organic load from the liquid phase. However, the high % of COD removal in R1-CF was not balance by a high percentage of methane since the produced methane at that time (end of cycle B) found to be only 36% of the initial COD. Renewal of the organic load on 31d (start of cycle C) with the same BW content further decreased the removal of dCOD, indicating that the performance of the three materials is reduced over time (**Supplementary Figures S1–S3**). Indeed, at the end of the experiment, the range found to be between 31.9 (R1-CF) and 35.6% (R2-CC) demonstrated ineffective microbial activity.

A first-order kinetic equation was fitted to COD concentration profiles at each experimental cycle, and the removal rate constants (k), the half-life values ($t_{1/2}$) and the correlation coefficients (R2) were calculated using the software GraphPad Prism 5 (**Table 1**). According to the results, the half-life values ranged between 6.2d (R2-CF, cycle A) and 29.1d (R1-CC, cycle C), indicating that as time passes, the performance of the reactors reduces. The F-test in the Graphpad prism showed that the rate constants and the half-lives were similar for all the reactors for a given cycle. No statistically significant differences existed despite the use of different electrodes. *p* values were 0.9220, 0.0733 and 0.0783 for cycles A, B and C, respectively.

Regarding the methane produced, this accounts for 27.6, 38.8, 51.5, and 62.5% of the total COD for R0, R1, R2 and R3, respectively. Part of the higher CH_4 produced in MEC reactors could be due to the hydrogen produced in the cathode and the utilization by hydrogenotrophic methanogens.

Soluble microbial products (SMPs) are widely classified as biomass-associated products (BAP-due to cell lysis) and utilization-associated products (UAP-which are produced during catabolism/anabolism) (Soh et al., 2021). The SMPs at the end of cycle 1 were higher for the control bioreactor than for the MEC-AC (**Figure 4**). However, the SMPs are built up and increased in all bioreactors at the end of the following cycles. The SMPs in cycles 2 and 3 were higher than in the first cycle; SMPs might be increased due to the higher bilge concentration in the second and third cycles. The SMPs remained higher in control bioreactor than in the other three MEC-ACs. The SMPs that could be recalcitrant organic compounds could have inhibited the anaerobic microorganisms, which is likely the reason for the lower performance in the third cycle compared to the first cycle.

VFAs Analysis

Chromatographic analysis of liquid samples for VFAs detection is presented in **Figure 5**. Regarding the different types of analyzed VFAs, acetic, propionic and valeric acid were only detected. During experimental cycle A, all three acids were present at concentrations between 26 and 573 mg L^{-1}. While the percentage of BW was increased from 50 to 75% moving from cycle A to B, both propionic and acetic acid were present. Their values were found to be up to 228 (R0-C) and 163 (R1-CF) mg L^{-1} for acetic and propionic acid, respectively. However, after the first two to 4 days of cycle B no acetic acid was detected, indicating its utilization by acetoclastic methanogens (Yu et al., 2016). Propionic acid was the only detectable compound until the end of cycle C (52d), and its concentrations over time varied from 26 (R1-CF) to 279 mg L-1 (R0-C) (**Supplementary Figure S4**).

At the end of the first cycle, the diluted bilge was biodegraded to acetic acid by acidogenic and acetogens microorganisms. The rate-limiting step was the acetoclastic methanogens. However, at cycles B and C, high propionic acid in an anaerobic bioreactor

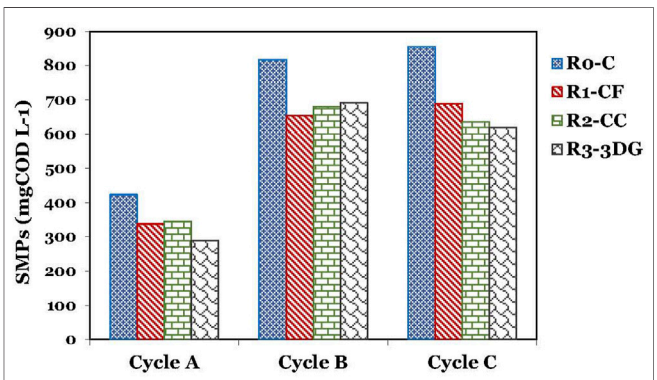

FIGURE 4 | Production of Soluble Microbial Products (SMPs) at the end of each experimental cycle A, B and C.

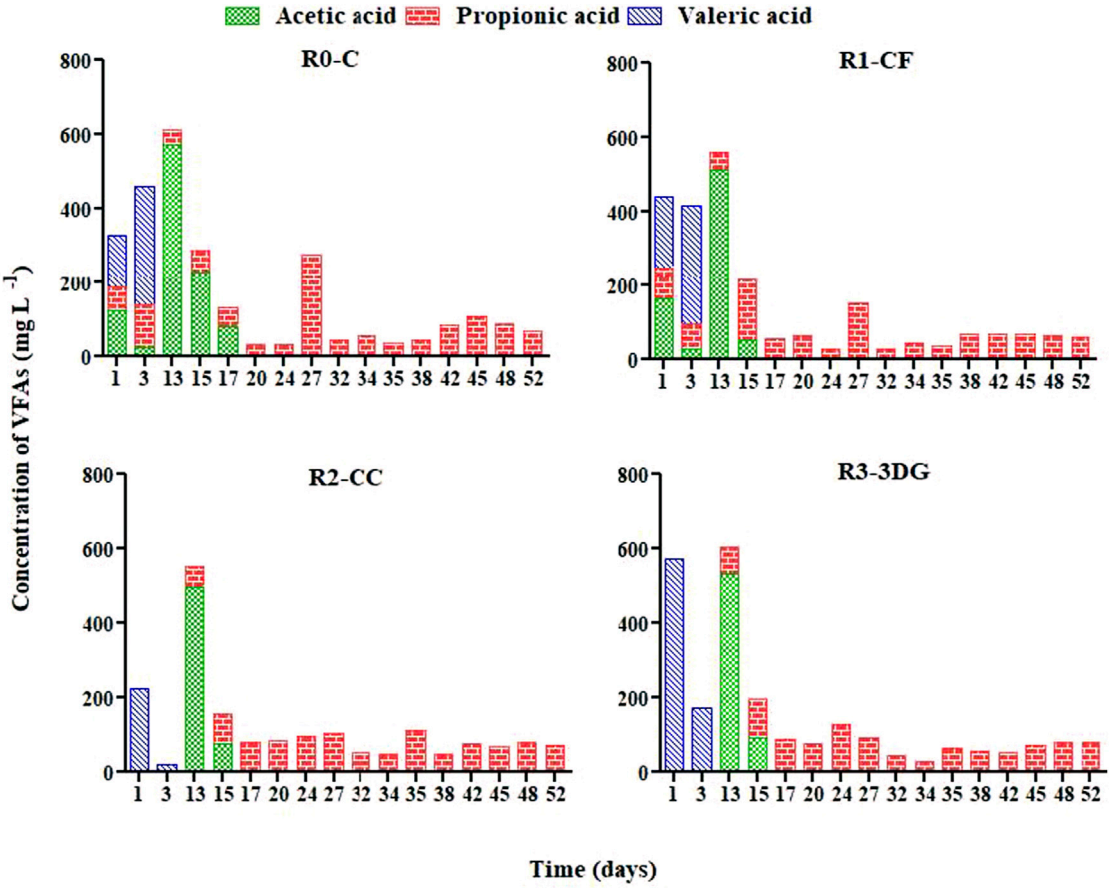

FIGURE 5 | Variation in VFAs composition (mg L^{-1}) over time in the different reactors during the three consecutive cycles.

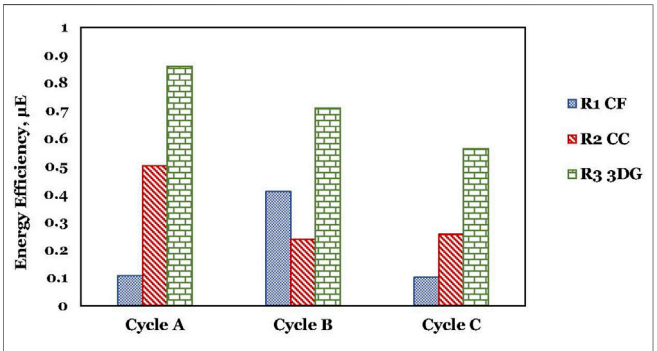

FIGURE 6 | Energy efficiency (μE) for three consecutive cycles in the different reactors.

indicated low performance, and its biodegradation required low hydrogen partial pressure (Yu et al., 2016). The higher percentage of bilge at these cycles inhibited hydrogen utilizing microorganisms such as hydrogenotrophic methanogens and homoacetogens, and therefore, the propionic acid utilization was not thermodynamically favorable (Charalambous and Vyrides 2021).

Energy Efficiency

The energy efficiency for the three MEC bioreactors is shown in **Figure 6**. Over the three cycles, R3 showed a higher efficiency compared to R1 and R2. However, the highest efficiency for R3 was only 0.86; this means that the incremental methane yield produced in the MEC cannot cover the electrical energy consumed in MEC. Even so, MEC-AD performance was better than the control, but the recalcitrant nature of bilge water did not allow the system to balance the consumed energy. From cycle 1 to cycle 3, as the SMPs increased, the energy efficiency decreased, probably due to the toxic compounds in bilge and of SMPs towards anaerobic microorganisms. In a similar system using MEC with commercial iron rods electrodes (Gatidou et al., 2022), an efficiency of 0.23 was found. Therefore, using carbon electrodes in MEC pointed out higher performance than the use of iron electrodes. The highest energy efficiency was for R3-3DG.

Microbial Profile

Regarding archaeal communities, the diversity of *Euryarchaeota* was the most abundant phylum in all samples (**Figure 7**). *Methanobacterium*, a typical hydrogen-utilizing methanogen that uses H_2 as an electron donor and CO_2 as an acceptor,

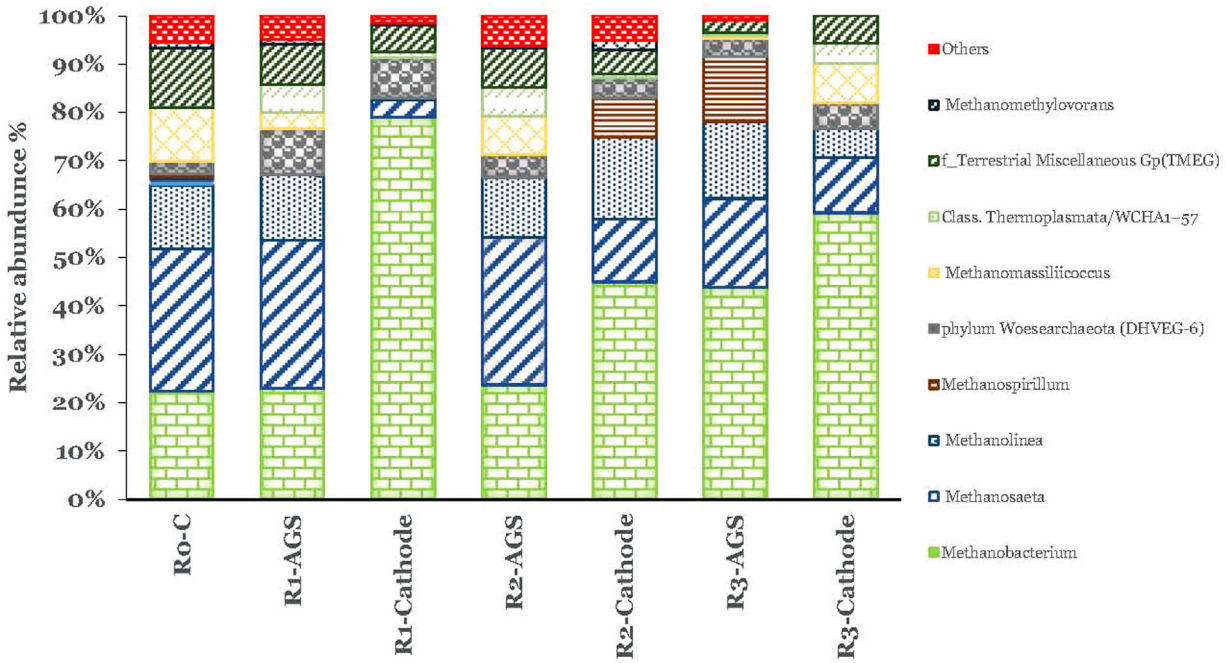

FIGURE 7 | The most abundant archaeal genera identified in the suspended sludge and on the cathodes.

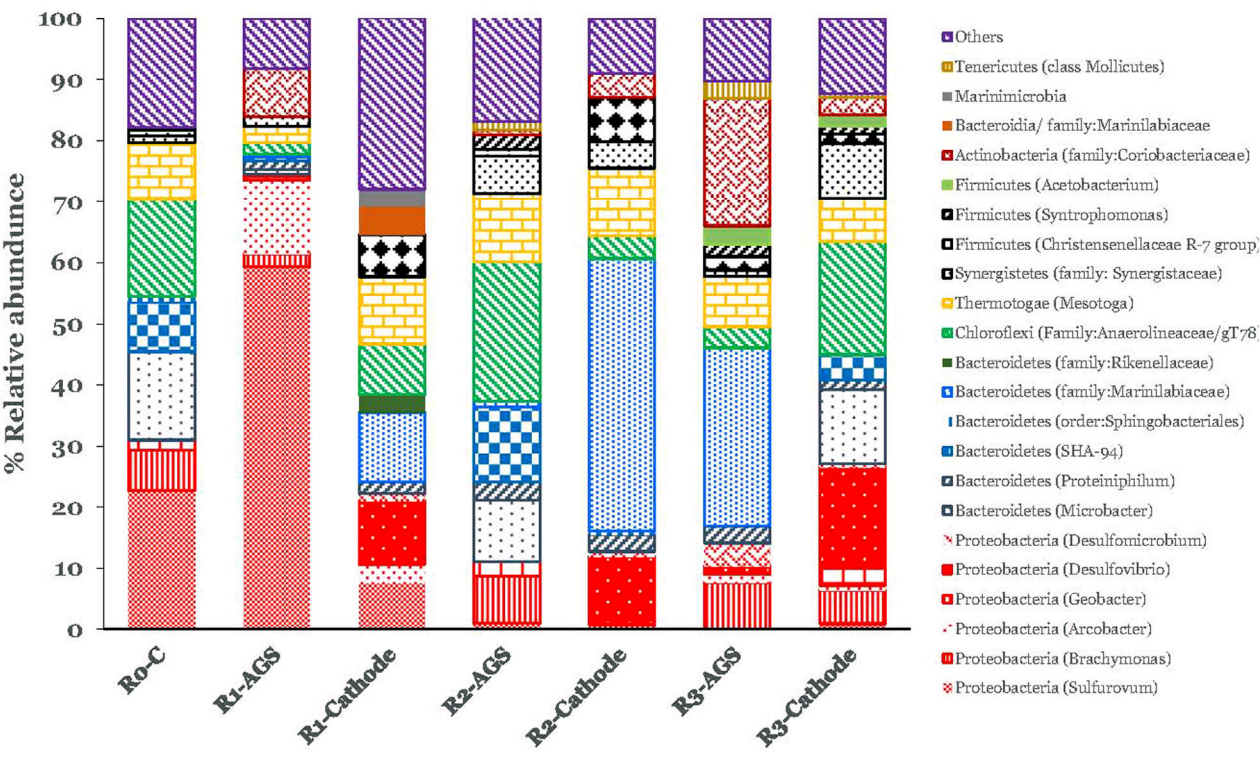

FIGURE 8 | Identified relative abundance at the bacterial community at the phylum and genus level in the bioreactors in the suspended sludge and on the cathodes.

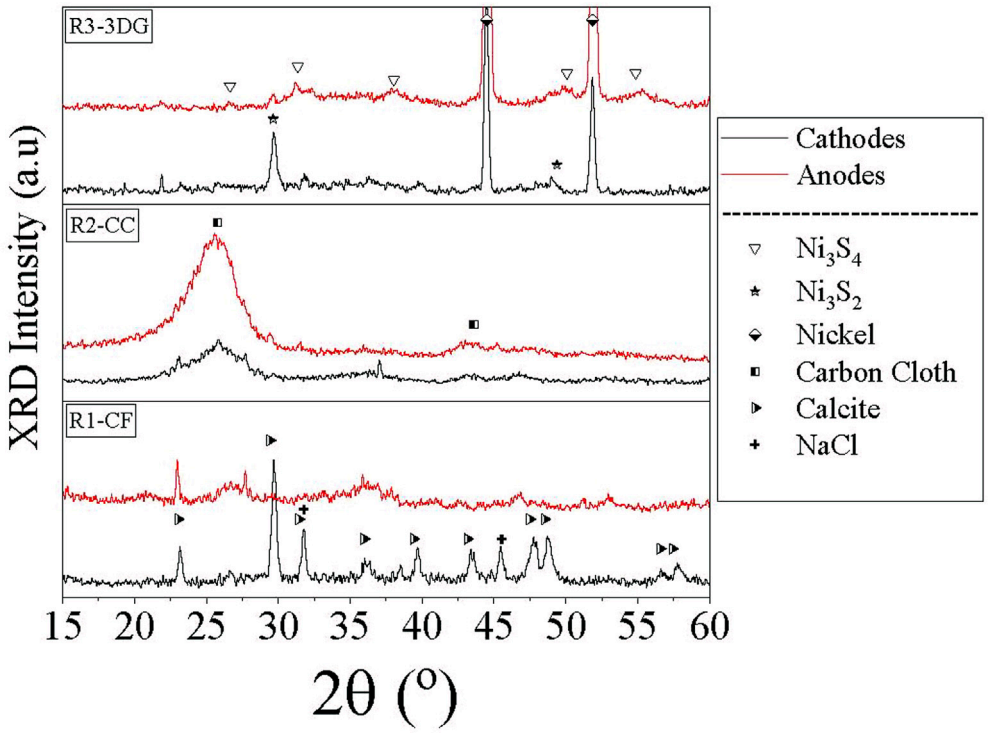

FIGURE 9 | XRD patterns of anodes (red lines) and cathodes (black lines) for the three types of electrodes (R1: carbon foam, R2: carbon Cloth, R3: 3-dimensional graphene).

was significantly higher in the cathodes than in the suspended AGS. At the carbon foam cathode, the relative abundance of *Methanobacterium* found to be 79.2%, whereas at the suspended AGS, this was around 23.9%. On the contrary, the relative abundance of *Methanosaeta* found to be only 3.6% and was significantly higher in the suspended sludge (30.8%). The same trend was observed in R2-CC and R3-3DG systems but the difference was not so pronounced (**Figure 7**). The results follow Siegert et al. (2015), who reported cathodes' attachment mainly by the genus *Methanobacterium* while studying methane production in acetate-fed MECs systems. In addition, hydrogenotrophic *Methanolinea* was found in similar relative abundance to all samples; it is exclusively found in microbial communities enriched with syntrophic substrates and is likely to play a role in propionic biodegradation.

Methanosaeta, an acetoclastic methanogen, was more abundant in the suspended AGS (**Figure 7**) and has been suggested as one of the prominent microbial groups responsible for methanogenic granule formation (Andronikou et al., 2022). Previous work (Gatidou et al., 2022) with MECs using iron rode electrodes also revealed high abundance of *Methanosaeta* in suspended sludge compared to the electrode surface.

Regarding the bacteria diversity, *Desulfovibrio* was identified at higher percentage in the cathodes compared to the suspended AGS. According to Carmona-Martínez et al. (2015) several microorganisms within the deltaproteobacteria class have been proved to possess electroactivity. This genus was also identified on iron rod electrodes during MEC treating bilge water (Gatidou et al., 2022). Apart from *Desulfovibrio* no other clear trend was detected among the different cathodes and the suspended AGS (**Figure 8**). However, the genus *Mesotoga* was found in all samples (**Figure 8**). This is in line with the findings of Mazioti A. A. et al. (2021) and Gatidou et al. (2022) that also exposed AGS to bilge water. Nesbø et al. (2019) reported that *Mesotoga* are frequently identified in oil-polluted marine mesophilic anaerobic environments. *Mesotoga*, although they belong to the thermophilic phylum of *Thermotogae*, are the only strictly mesophilic genus (Pollo et al., 2015) and may take part in syntrophic acetate limitation (Nobu et al., 2015).

Anaerolineaceae (T78) was also found in all samples and the highest relative abundance was observed in the suspended AGS of R2-CC (**Figure 8**). *Anaerolineales* family can maintain the physical integrity of the anaerobic granular structure (Zhu et al., 2017). Furthemore, this specific species found to be the most dominant group of bacteria in a semi-continuous anaerobic digester treated lipid wastewater (Nakasaki et al., 2020). *Marinilabiaceae* was identified only at high relative abundance in R1-CF and R2-CC cathodes (**Figure 8**) but not in R3-3DG. The family *Marinilabiaceae* are an anaerobic mesophilic bacterium that can ferment various substrates and produce propionate, acetate, and succinate (Poirier et al., 2017).

Electrodes Analysis

Despite the difficulties that occurred during electrodes XRD analysis, some initial conclusions were still possible to draw. As shown in **Figure 9**, XRD pattern of R1-CF cathode (carbon foam material) revealed the characteristic peaks of calcite ($CaCO_3$) and halite (NaCl). Formation of $CaCO_3$ was probably due to biomineralization by the bacterial metabolic activity which resulted in mineral precipitation and growth (Keren-Paz and Kolodkin-Gal, 2020). Mazioti A. A. et al. (2021) also observed the formation of $CaCO_3$ in biocarrier during BW treatment. However, it is also possible that the formation of CaCO3 was caused due to the slight increase of pH (7.72 at the end of cycle C). According to the literature (Zeppilli et al., 2021; Ceballos-Escalera et al., 2022), increase of pH near cathode enhances the precipitation of cations like Ca^{+2} leading to overlap of biofilm and electrode surface. This fact negatively affects the operation of the MEC system decreasing the effectiveness of the treatment.

NaCl obviously came from seawater content in BW. The presence of calcite on the surface of the electrode may have reduced the available surface area of the electrode contributing to its lower performance. On the contrary, the XRD pattern of the anode consisted of a messy set of low intensity and broad peaks which was unable to assign to a specific crystalline phase.

Regarding CC material, both electrodes of R2-CC reactor exhibited only the characteristic broad peaks of carbon cloth at 25.8° and 43.6° 2θ.

As for R3-3DG, the XRD patterns revealed the presence of Ni_3S_4 and Ni_3S_2 in the anode and cathode, respectively. The formation of nickel sulfides could be attributed to the oxidation of 3DG and especially the nickel foam template by HS^- released from sulfur compounds that were contained in the BW. Moreover, both electrodes exhibited pure metallic Ni peaks due to the nickel foam used for their synthesis, while in the cathode some minor unidentified peaks were also observed. The presence of sulfides is in line with the microbial profile findings and the high relative abundance of *Desulfovibrio* in the cathode of R3-3DG.

CONCLUSION

Single-chamber MEC-AGS reactors used to treat real bilge water revealed higher methane production than the control (AGS reactor) in all experimental cycles. The performance of the three types of electrodes investigated in the present study for the first time was significantly affected by time and organic load content. 3DG was more effective at lower BW concentrations and generated higher CH_4 production among the different materials examined. On the contrary, carbon foam demonstrated better resistance at higher BW content during the second cycle. As for CC performance, results indicated the existence of a ceiling on methane production regardless of the BW concentration or operation time. Considerable COD removal was observed in all MECs, confirming the benefit of using them. However, as the organic load content was increased the biomass seemed to be distressed mainly in the R2-CC and R3-3DG reactors (third cycle). VFAs analysis demonstrated the presence of acetic, propionic and valeric acid, but as the percentage of BW was increased, propionic acid was dominated. The energy efficiency was higher for the system with 3DG electrode than the other systems; however, the methane energy produced in the MECs cannot cover the electrical energy consumed in MECs. Results regarding DNA sequencing analysis indicated the higher predominance of *Methanobacterium* and *Desulfovibrio* in the cathodes compared to suspended AGS. Additionally, the XRD analysis of used electrodes confirmed the formation of calcite ($CaCO_3$) and halite (NaCl) on the R1-CF cathode. At R3-3DG, the presence of Ni_3S_4 and Ni_3S_2 in the anode and cathode were identified.

DATA AVAILABILITY STATEMENT

The original contributions presented in the study are included in the article/**Supplementary Material**, further inquiries can be directed to the corresponding authors.

AUTHOR CONTRIBUTIONS

GG: Investigation, Methodology, Validation, Visualization, Writing- Original draft preparation. MC: Investigation, Validation. LK: Investigation. GC: Conceptualization, Methodology, Visualization, Project administration, Supervision, Writing - Review and Editing. IV: Conceptualization, Methodology, Visualization, Project administration, Supervision, Writing - Review and Editing. All authors contributed to the article and approved the submitted version.

FUNDING

The work has received funding from the European Union's Horizon 2020 research and innovation programme under the Marie Sklodowska-Curie grant agreement No 841797. Synthesis and characterization of carbon-based electrodes was conducted using support from the project POST-DOC/0718/0213 which is co-funded by the European Regional Development Fund and the Republic of Cyprus through the Research and Innovation Foundation.

ACKNOWLEDGMENTS

The authors would like to clarify that Ecofuel Ltd. (Cyprus) had no role in study funding, design, data collection and analysis, decision to publish or preparation of the current manuscript.

SUPPLEMENTARY MATERIAL

The Supplementary Material for this article can be found online at: https://www.frontiersin.org/articles/10.3389/fenvs.2022.894240/full#supplementary-material

REFERENCES

Ahmadi, M., Jorfi, S., Kujlu, R., Ghafari, S., Darvishi, R., Soltani, Ch., et al. (2017). A Novel Salt-Tolerant Bacterial Consortium for Biodegradation of Saline and Recalcitrant Petrochemical Wastewater. *J. Environ. Manage.* 191, 198–208. doi:10.1016/j.jenvman.2017.01.010

Andronikou, M., Adamou, V., Koutsokeras, L., Constantinides, G., and Vyrides, I. (2022). Magnesium Ribbon and Anaerobic Granular Sludge for Conversion of CO_2 to CH_4 or Biogas Upgrading. *Chem. Eng. J.* 435, 134888. doi:10.1016/j.cej.2022.134888

Angelidaki, I., Alves, M., Bolzonella, D., Borzacconi, L., Campos, J. L., Guwy, A. J., et al. (2009). Defining the Biomethane Potential (BMP) of Solid Organic Wastes and Energy Crops: a Proposed Protocol for Batch Assays. *Water Sci. Technol.* 59 (5), 927–934. doi:10.2166/wst.2009.040

Carmona-Martínez, A. A., Trably, E., Milferstedt, K., Lacroix, R., Etcheverry, L., and Bernet, N. (2015). Long-term Continuous Production of H2 in a Microbial Electrolysis Cell (MEC) Treating Saline Wastewater. *Water Res.* 81, 149–156. doi:10.1016/j.watres.2015.05.041

Cazoir, D., Fine, L., Ferronato, C., and Chovelon, J.-M. (2012). Hydrocarbon Removal from Bilgewater by a Combination of Air-Stripping and Photocatalysis. *J. Hazard. Mater.* 235-236, 159–168. doi:10.1016/j.jhazmat.2012.07.037

Ceballos-Escalera, A., Pous, N., Balaguer, M. D., and Puig, S. (2022). Electrochemical Water Softening as Pretreatment for Nitrate Electro Bioremediation. *Sci. Total Environ.* 806, 150433. doi:10.1016/j.scitotenv.2021.150433

Charalambous, P., and Vyrides, I. (2021). *In Situ* biogas Upgrading and Enhancement of Anaerobic Digestion of Cheese Whey by Addition of Scrap or Powder Zero-Valent Iron (ZVI). *J. Environ. Manag.* 280, 111651. doi:10.1016/j.jenvman.2020.111651

Choi, O., and Sang, B. I. (2016). Extracellular Electron Transfer from Cathode to Microbes: Application for Biofuel Production. *Biotechnol. Biofuels* 9 (1), 11–14. doi:10.1186/s13068-016-0426-0

Gatidou, G., Samanides, C. G., Fountoulakis, M. S., and Vyrides, I. (2022). Microbial Electrolysis Cell Coupled with Anaerobic Granular Sludge: A Novel Technology for Real Bilge Water Treatment. *Chemosphere* 296, 133988. doi:10.1016/j.chemosphere.2022.133988

Hwang, J.-H., Kim, K.-Y., Resurreccion, E. P., and Lee, W. H. (2019). Surfactant Addition to Enhance Bioavailability of Bilge Water in Single Chamber Microbial Fuel Cells (MFCs). *J. Hazard. Mater.* 368, 732–738. doi:10.1016/j.jhazmat.2019.02.007

Hwang, J.-H., Ryu, H., Rodriguez, K. L., Fahad, S., Domingo, J. S., Kushima, A., et al. (2021). A Strategy for Power Generation from Bilgewater Using a Photosynthetic Microalgal Fuel Cell (MAFC). *J. Power Sources* 484, 229222. doi:10.1016/j.jpowsour.2020.229222

Keren-Paz, A., and Kolodkin-Gal, I. (2020). A Brick in the Wall: Discovering a Novel Mineral Component of the Biofilm Extracellular Matrix. *New Biotechnol.* 56, 9–15. doi:10.1016/j.nbt.2019.11.002

Khan, M. S., Lu, F., Kashif, M., and Shen, P. (2021). Multiple Effects of Different Nickel Concentrations on the Stability of Anaerobic Digestion of Molasses. *Sustainability* 13 (9), 4971. doi:10.3390/su13094971

Krishnamurthy, A., Gadhamshetty, V., Mukherjee, R., Chen, Z., Ren, W., Cheng, H.-M., et al. (2013). Passivation of Microbial Corrosion Using a Graphene Coating. *Carbon* 56, 45–49. doi:10.1016/j.carbon.2012.12.060

Ma, X.-Ch., Li, X.-K., Wang, X.-W., Liu, G.G., Zuo, J. L., Wang, S.-T., et al. (2020). Impact of Salinity on Anaerobic Microbial Community sStructure in High Organic Loading Purified Terephthalic Acid Wastewater Treatment System. *J. Hazard. Mater.* 383, 121132. doi:10.1016/j.jhazmat.2019.121132

Mansoorian, H. J., Mahvi, A., Nabizadeh, R., Alimohammadi, M., Nazmara, S., and Yaghmaeian, K. (2020). Evaluating the Performance of Coupled MFC-MEC with Graphite felt/MWCNTs Polyscale Electrode in Landfill Leachate Treatment, and Bioelectricity and Biogas Production. *J. Environ. Health Sci. Eng.* 18 (2), 1067–1082. doi:10.1007/s40201-020-00528-2

Mao, S., Lu, G., and Chen, J. (2015). Three-Dimensional Graphene-Based Composites for Energy Applications. *Nanoscale* 7, 6924–6943. doi:10.1039/C4NR06609J

Mazioti, A. A., Koutsokeras, L. E., Constantinides, G., and Vyrides, I. (2021b). Untapped Potential of Moving Bed Biofilm Reactors with Different Biocarrier Types for Bilge Water Treatment: A Laboratory-Scale Study. *Water* 13, 13131810. doi:10.3390/w13131810

Mazioti, A. A., Vasquez, M. I., and Vyrides, I. (2021a). Comparison of Different Cultures and Culturing Conditions for the Biological Deterioration of Organic Load from Real Saline Bilge Wastewater: Microbial Diversity Insights and Ecotoxicity Assessment. *Environ. Sci. Pollut. Res.* 28 (27), 36506–36522. doi:10.1007/s11356-021-13153-9

McLaughlin, C., Falatko, D., Danesi, R., and Albert, R. (2014). Characterizing Shipboard Bilgewater Effluent before and after Treatment. *Environ. Sci. Pollut. Res.* 21, 5637–5652. doi:10.1007/s11356-013-2443-x

Mei, X., Wang, H., Hou, D., Lobo, F. L., Xing, D., and Ren, Z. J. (2019). Shipboard Bilge Water Treatment by Electrocoagulation Powered by Microbial Fuel Cells. *Front. Environ. Sci. Eng.* 13 (4), 1–7. doi:10.1007/s11783-019-1134-3

Mier, A. A., Olvera-Vargas, H., Mejía-López, M., Longoria, A., Verea, L., Sebastian, P. J., et al. (2021). A Review of Recent Advances in Electrode Materials for Emerging Bioelectrochemical Systems: From Biofilm-Bearing Anodes to Specialized Cathodes. *Chemosphere* 283, 131138. doi:10.1016/j.chemosphere.2021.131138

Nakasaki, K., Nguyen, K. K., Ballesteros, F. C., Jr, Maekawa, T., and Koyama, M. (2020). Characterizing the Microbial Community Involved in Anaerobic Digestion of Lipid-Rich Wastewater to Produce Methane Gas. *Anaerobe* 61, 102082. doi:10.1016/j.anaerobe.2019.102082

Nesbø, C. L., Charchuk, R., Pollo, S. M. J., Budwill, K., Kublanov, I. V., Haverkamp, T. H. A., et al. (2019). Genomic Analysis of the Mesophilic Thermotogae Genus Mesotoga Reveals Phylogeographic Structure and Genomic Determinants of its Distinct Metabolism. *Environ. Microbiol.* 21 (1), 456–470. doi:10.1111/1462-2920.14477

Nobu, M. K., Narihiro, T., Rinke, C., Kamagata, Y., Tringe, S. G., Woyke, T., et al. (2015). Microbial Dark Matter Ecogenomics Reveals Complex Synergistic Networks in a Methanogenic Bioreactor. *Isme J.* 9 (8), 1710–1722. doi:10.1038/ismej.2014.256

Poirier, S., Madigou, C., Bouchez, T., and Chapleur, O. (2017). Improving Anaerobic Digestion with Support Media: Mitigation of Ammonia Inhibition and Effect on Microbial Communities. *Bioresour. Technol.* 235, 229–239. doi:10.1016/j.biortech.2017.03.099

Pollo, S. M. J., Zhaxybayeva, O., and Nesbø, C. L. (2015). Insights into Thermoadaptation and the Evolution of Mesophily from the Bacterial Phylum Thermotogae. *Can. J. Microbiol.* 61 (9), 655–670. doi:10.1139/cjm-2015-0073

Siegert, M., Li, X.-F., Yates, M. D., and Logan, B. E. (2015). The Presence of Hydrogenotrophic Methanogens in the Inoculum Improves Methane Gas Production in Microbial Electrolysis Cells. *Front. Microbiol.* 5, 778. doi:10.3389/fmicb.2014.00778

Soh, Y. N. A., Kunacheva, C., Menon, S., Webster, R. D., and Stuckey, D. C. (2021). Comparison of Soluble Microbial Product (SMP) Production in Full-Scale Anaerobic/aerobic Industrial Wastewater Treatment and a Laboratory Based Synthetic Feed Anaerobic Membrane System. *Sci. Total Environ.* 754, 142173. doi:10.1016/j.scitotenv.2020.142173

Tiselius, P., and Magnusson, K. (2017). Toxicity of Treated Bilge Water: The Need for Revised Regulatory Control. *Mar. Pollut. Bull.* 114 (2), 860–866. doi:10.1016/j.marpolbul.2016.11.010

Vyrides, I., Drakou, E.-M., Ioannou, S., Michael, F., Gatidou, G., and Stasinakis, A. S. (2018). Biodegradation of Bilge Water: Batch Test under Anaerobic and Aerobic Conditions and Performance of Three Pilot Aerobic Moving Bed Biofilm Reactors (MBBRs) at Different FIlling Fractionsfilling Fractions. *J. Environ. Manag.* 217, 356–362. doi:10.1016/j.jenvman.2018.03.086

Vyrides, I., and Stuckey, D. C. (2009). Effect of Fluctuations in Salinity on Anaerobic Biomass and Production of Soluble Microbial Products (SMPs). *Biodegradation* 20 (2), 165–175. doi:10.1007/s10532-008-9210-6

Xing, T., Yun, S., Li, B., Wang, K., Chen, J., Jia, B., et al. (2021). Coconut-shell-derived Bio-Based Carbon Enhanced Microbial Electrolysis Cells for Upgrading Anaerobic Co-digestion of Cow Manure and Aloe Peel Waste. *Bioresour. Technol.* 338, 125520. doi:10.1016/j.biortech.2021.125520

Yu, F., Wang, C., and Ma, J. (2016). Applications of Graphene-Modified Electrodes in Microbial Fuel Cells. *Materials* 9 (10), 807. doi:10.3390/ma9100807

Zeng, X., Borole, A. P., and Pavlostathis, S. G. (2016). Inhibitory Effect of Furanic and Phenolic Compounds on Exoelectrogenesis in a Microbial Electrolysis Cell

Bioanode. *Environ. Sci. Technol.* 50 (20), 11357–11365. doi:10.1021/acs.est.6b01505

Zeppilli, M., Paiano, P., Torres, C., and Pant, D. (2021). A Critical Evaluation of the pH Split and Associated Effects in Bioelectrochemical Processes. *Chem. Eng. J.* 422, 130155. doi:10.1016/j.cej.2021.130155

Zhu, X., Kougias, P. G., Treu, L., Campanaro, S., and Angelidaki, I. (2017). Microbial Community Changes in Methanogenic Granules during the Transition from Mesophilic to Thermophilic Conditions. *Appl. Microbiol. Biotechnol.* 101 (3), 1313–1322. doi:10.1007/s00253-016-8028-0

Conflict of Interest: The authors declare that the research was conducted in the absence of any commercial or financial relationships that could be construed as a potential conflict of interest.

Publisher's Note: All claims expressed in this article are solely those of the authors and do not necessarily represent those of their affiliated organizations, or those of the publisher, the editors and the reviewers. Any product that may be evaluated in this article, or claim that may be made by its manufacturer, is not guaranteed or endorsed by the publisher.